A Microstructural Study of Carbon Fibers for Space Applications

David P. Anderson and Allan S. Crasto

University of Dayton Research Institute,
300 College Park Avenue
Dayton, Ohio 45469-0168

INTRODUCTION

Advanced composites are used in space applications because of their high specific stiffness and strength, high thermal conductivity, and near-zero coefficient of thermal expansion (CTE). Attractive reinforcing fiber properties for these composites are a high specific modulus to minimize component weight, a high thermal conductivity to allow efficient thermal management through rapid dissipation of heat, and a negative axial CTE to allow composite CTE tailorability for dimensional stability in the thermal environment of space. This mix of properties is available in high-modulus pitch-based carbon fibers. Inherent in these fibers, however, is a relatively lower tensile strength and significantly lower compression strength compared to their PAN-based counterparts which, combined with the high stiffness, produce poor handleability and spreadability.

A number of high modulus pitch-based carbon fibers have been developed in Japan with better strength properties than their domestic counterparts, including the state-of-the-art high thermal conductivity fiber, Amoco's K-1100. These fibers have been matched with a recently developed P-100 XHT fiber from AMOCO. This study was undertaken to examine the microstructural features in several of these fibers to gain an understanding of the correlations between microstructure, mechanical properties, and conductivity.

EXPERIMENTAL

Commercially available pitch-based carbon fibers were used in this study. These include the P-series, K-1100, and newer P-100 XHT from AMOCO; E-series from DuPont; Dialead K- and Ku-series from Mitsubishi Kasei; FT-series from Tonen; and Nippon's XN-70A.

Electrical resistivity was measured by extending individual fibers on a glass plate under minimal tension and affixing their ends to the plate with sealing wax. Resistance was measured with a multimeter using silver paint to provide electrical contact to the lead wires. Fiber gage length was measured to the nearest 0.2 mm and fiber diameter was measured in an optical microscope with an image-splitting eyepiece.

For x-ray diffraction (XRD), the fiber bundles were mounted on a cardboard holder with cyanoacrylate glue. The bundles were scanned in symmetric transmission on a Huber 4-circle x-ray diffractometer. Incident beam crystal monochromated CuKα radiation (λ = 0.15418 nm) from a Rigaku RU-200 rotating anode generator, at a power of 45 kV and 70 mA, was the x-ray source. The data was corrected for absorption, polarization, incoherent scattering, and Lorentz factors. Curve fitting was used to get d-spacings and peak widths for determination of crystallite sizes [1,2]. Crystallite orientations were measured by obtaining the full-width at half maximum of an azimuthal scan of the (00,2) reflection.

SEM was performed on fiber ends using a Leica 360 field emission gun SEM. The fiber specimens were obtained by fracture of a fiber bundle in flexure.

RESULTS AND DISCUSSION

SEM micrographs of the high modulus fibers showed a wavy sheet pattern, typical of the pitch based carbon fibers [3]. The sheet size shows a correlation with the x-ray crystallite size determined by XRD although the sheets are significantly larger than the measured crystallites.

Thermal conductivity of the fibers was not determined in this study. However, excellent correlations have been reported between fiber electrical and thermal conductivity for a large number of pitch-based carbon fibers [4-6]. This is to be expected since both properties are reported to be based on the same mechanism [5]. Consequently, fibers for which the thermal conductivity is unknown are assumed to follow the established correlation The thermal conductivities of the remaining fibers were taken from the technical literature [4,5]. X-ray data were correlated with electrical resistivity, thermal conductivity and manufacturer's mechanical data.

The high axial conductivity in carbon fibers is a result the inherently high conductivity of the graphene a-b plane and alignment of these planes along the fiber axis. Connection points between crystallites are a source of resistance; the larger the crystallite size the fewer there are of these connections and, consequently, the conductivity should be higher. The fibers in this study follow this correlation as seen from the plot in Figure 1. Crystallite size generally shows an inverse correlation with d-spacing, with higher degrees of graphitization promoting larger crystallites with closer-packed graphitic planes. Figure 2 shows an almost linear increase in resistivity with $d_{(00,2)}$ up to the point where the graphitic planes assume a fully turbostratic arrangement ($d_{(00,2)}$ = 0.344 nm.).

As expected, the fiber tensile modulus correlates well with crystallite orientation (Figure 3). The microstructural feature which appears to provide the best correlation with fiber compression strength is crystallite size (Figure 4), with smaller crystals leading to higher compression strengths. Fiber tensile strength, on the other hand, does not show a good correlation with any microstructural parameter. These correlations between mechanical properties and microstructure are consistent with our previous work [3,7-9].

The new P-100 XHT fiber from AMOCO has an 80% higher tensile strength and a 30% higher compressive strength

than its predecessor, P-100, but has the same tensile modulus. It differs microstructurally from P-100 in that it has a 40% lower degree of graphitization and 30% smaller crystallite size. Crystallite orientation and size, as well as degree of graphitization, generally increase with heat treatment. It appears, therefore, that the crystallite orientation required for the high modulus of P-100 XHT is not achieved through heat treatment alone (which would have raised the degree of graphitization and crystallite size to the level seen in P-100) but by appropriate changes in other processing parameters. The smaller crystallite size explains the higher compressive strength of P-100 XHT. Improvements in tensile strength may correlate with increased purity of the pitch precursor to reduce the defects in the final fibers.

CONCLUSIONS

The processing of high modulus carbon fibers with lower degrees of graphitization (higher $d_{(00,2)}$) produces fibers with better compressive strengths but with higher electrical resistivity (or correspondingly lower axial thermal conductivity). Improvements in fiber compressive strength can be made without sacrificing fiber stiffness, as demonstrated by comparison of P-100 and P-100 XHT. On the other hand, it appears that fiber thermal conductivity and compression strength are inversely related with an increase in one property coming at the expense of the other. This relationship must be borne in mind when selecting a fiber for a thermal-structural application in space.

ACKNOWLEDGMENTS

This work was supported by the U.S. Air Force, Wright Laboratories, Materials Directorate under contract no. F33615-91-C-5618.

REFERENCES

1. P. Scherrer, *Gottinger Nachrichten*, **2**, 98 (1918).
2. W. Ruland, *Acta Cryst.*, **22**, 615 (1967).
3. A. S. Crasto and D. P. Anderson, *Proc. ASC Tech. Conf.*, **5**, 809 (1990).
4. L. Piraux, J.-P. Issi, and P. Coopmans, *Measurement*, **5**, 2 (1987).
5. B. Nysten, J.-P. Issi, R. Barton, Jr., D. R. Boyington, and J. G. Lavin, *Physical Review B*, **44**, 2142 (1991).
6. J. G. Lavin, D. R. Boyington, J. Lahijani, B. Nysten, and J.-P. Issi, *Carbon*, **31**, 1001 (1993).
7. D. P. Anderson and S. Kumar, *Proc. of SPE ANTEC-90*, 1248 (1990).
8. S. Kumar, V. Mehta, D. P. Anderson, and A. S. Crasto, *Proc. 37th Int'l SAMPE Symp.*, 967 (1992).
9. Satish Kumar, D. P. Anderson, and A. S. Crasto, *J. Mat. Sci.*, **28**, 423 (1993).

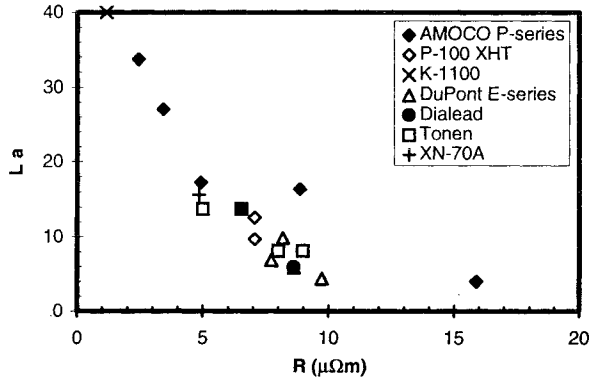

Figure 1. In-plane graphitic crystal size parallel to the fiber axis, L_a, and electrical resistivity, R, in carbon fibers.

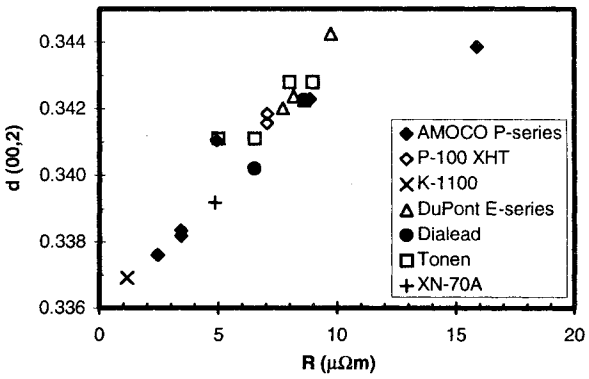

Figure 2. Spacing between graphene planes, $d_{(00,2)}$, and electrical resistivity, R, in carbon fibers.

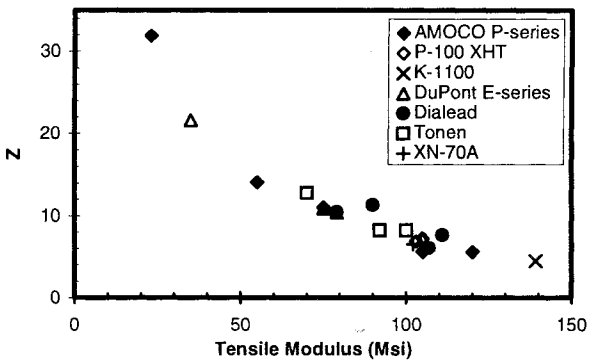

Figure 3. Fiber c-axis orientation, Z, and carbon fiber tensile modulus.

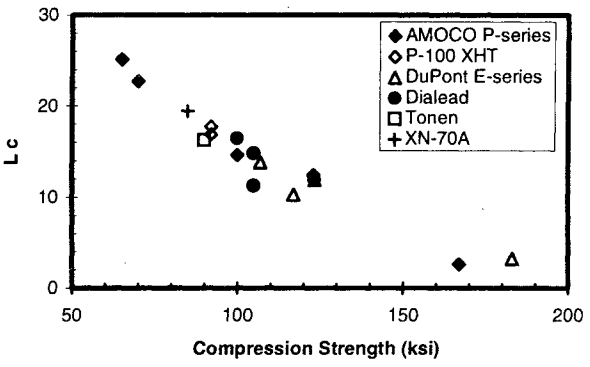

Figure 4. C-axis crystallite size, L_c, and carbon fiber compression strengths.